

Non-linearity of flexion–extension characteristics in spinal segments

HANS NÄGERL¹, THELONIUS HAWELLEK¹, ANDREA LEHMANN¹, JAN HUBERT¹, JULIA SAPTSCHAK¹,
JOCHEN DÖRNER², BJÖRN WERNER RAAB³, JOCHEN FANGHÄNEL⁴, DIETMAR KUBEIN-MEESENBURG¹,
MARTIN MICHAEL WACHOWSKI^{5,*}

¹Department of Orthodontics, University of Göttingen, Germany.

²Orthopaedic Clinic, Northeim, Germany.

³Department of Radiology, University of Göttingen, Germany.

⁴Department of Oral Anatomy, University of Greifswald, Germany.

⁵Department of Trauma Surgery, Plastic and Reconstructive Surgery, University of Göttingen, Germany.

Spinal biomechanics is still known just fragmentary since the only description by angle-torque characteristics without simultaneous recording of migration of the instantaneous helical axis (IHA) is not sufficient. Time-dependent flexion/extension following a cyclic laterally directed torque was measured at all six degrees of freedom by a highly precise custom-made 6D apparatus. In order to enhance the localizing resolution of IHA migration as the function of the flexional/extensional angle, small ranges of motion (ROM) were used at several degrees of pre-extension.

4 L3/L4, 3 L4/L5 and 2 T2/T3 human segments were investigated. In extensional motion, wide dorsal IHA-migrations were measured in lumbar segments and correlated with the distinct asymmetric shapes of the characteristics in extensional motion. The respective increase of differential stiffness could mainly be traced back to the enlarging geometrical moment of inertia of the segments by the dorsally migrating IHA. Both thoracic segments showed a predominant IHA-migration in cranial/caudal direction.

A simple model makes it evident that the opposite curvature morphology of lumbar and thoracic joint facets conditions the different directions of IHA migration.

Key words: spinal segments, extensional motion, nonlinearity, extensional/flexional characteristics, IHA-migration, stiffness increase

1. Introduction

Rotational angle–torque characteristics of human spinal segments show distinctive nonlinearity. As shown below in flexion/extension, the characteristics of L3/L4- and L4/L5-segments resemble “diode characteristics” known from electronics. The differential stiffness of the segments rapidly increases in extensional motion [1], [2]. This eye-catching *asymmetric* nonlinearity does not seem to be caused by the material of the intervertebral disc, since nonlinearity of material hardly depends on the direction of

flexional/extensional torque. This idea is supported by the well-known experience that segments with removed vertebral joints (VJ) show practically *symmetric* S-shaped characteristics [3], [4]. Therefore it seemed likely that the guidance by the VJ would affect the asymmetry of the flexional/extensional characteristics, since for geometrical reasons the joint facets come into contact under an extensional torque and uncouple in flexion. The differential stiffness of the segment increases, when in extension the joint guidance makes the instantaneous extensional/flexional rotational axis to migrate dorsally [4], [5]. This obvious mechanism can be supported

* Corresponding author: Martin Wachowski, Department of Trauma Surgery, Plastic and Reconstructive Surgery, University of Göttingen, Germany. E-mail:martin.wachowski@web.de

Received: January 4th, 2010

Accepted for publication: January 26th, 2010

by the following simple considerations: a segment consists of two rigid bodies joined by an elastic layer, the material of which may show Hookian behaviour (figure 1).

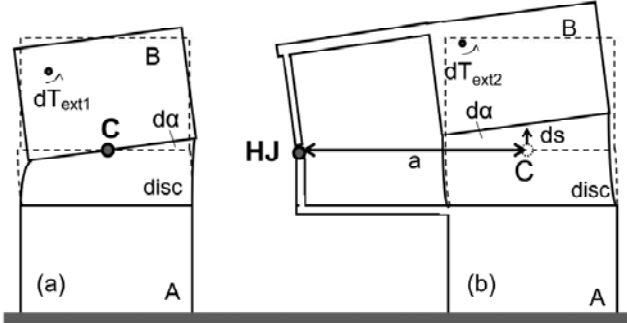


Fig. 1. Illustration of Steiner theorem: (a) two rigid bodies A and B are connected with an elastic layer. Extensional torque increment $dT_{\text{ext}1}$ produces rotational increment $d\alpha$ around axis C, (b) both bodies are additionally constrained by a hinge joint (HJ): to rotate body B around HJ by $d\alpha$ torque the increment $dT_{\text{ext}2}$ must be enhanced since body B is additionally displaced by increment ds

In the case (a), an extensional/flexional torque applied to the upper body B rotates it around the rotational axis C. The device would show a linear characteristic corresponding to the extensional/flexional stiffness D_{min} of the layer. Case (b): when, however, both bodies are additionally connected by a hinge joint (HJ), its constraint transfers the position of the rotational axis into the centre of the hinge. Thereby the geometric moment of inertia of the layer becomes enhanced: the extensional stiffness/flexional stiffness D of the layer must increase according to the theorem of Steiner [6], [7]:

$$D = D(a) = D_{\text{min}} + a^2 \cdot D_N \quad (1)$$

or

$$\Delta D(a)^{1/2} = (D(a) - D_{\text{min}})^{1/2} = D_N^{1/2} \cdot a.$$

$D(a)$ = instantaneous stiffness, D_{min} = minimal flexional/extensional stiffness, D_N = normal stiffness of the intervertebral disc, a = distance between position of the rotational axis in minimal stiffness (D_{min}) and in actual stiffness $D(a)$.

Hypotheses: a) the degree of dorsal IHA migration depends on the shape and alignment of the joint facets; b) is it that the IHA position migrates dorsally, the instantaneous stiffness of the segment would nearly increase according to the Steiner formula.

2. Material and method

Material: 4 L3/L4, 3 L4/L5, 2 Th2/Th3 human segments (age: 59.8 ± 16.6 years) were stabilized by a solution which did not alter the hardness and shape of the osseous and articular structures [8]. In this way, it was possible to ensure that the joints remained much harder than the intervertebral disc and the ligaments so that the predominance of the joints in guiding the segment was not affected by the preservation technique [9]. Abnormalities were excluded using X-ray images and CT scans.

Measuring apparatus: it has been described by MANSOUR et al. in detail [10]. Briefly: the position of the upper vertebra was monitored in relation to the lower vertebra. The 6 degrees of freedom tracking device consists of six inductive linear displacement sensors (1310 Mahr type, Göttingen, Germany), which have a resolution of 0.01–2.4 μm depending on gain. Their mounts were rigidly attached to the lower vertebra. The tips of the sensors were in contact with three glass plates, which were rigidly attached to the upper vertebra and form a cube. The sensors were arranged in a 3-2-1 configuration so that the positions of their tips define the momentary position of the cube, hence that of the moved coordinate system.

For the L4/L5 and Th2/Th3 segments an axially directed force F_z was applied adjusting its force line through the center of resistance so that the upper vertebra was neither laterally tilted nor flexed or extended (central position of F_z). In the L3/L4 segments, however, F_z ran in central position through the center of the spinal channel. When the position of the upper vertebra became stationary, the resulting position of the moved coordinate system was saved as the reference system.

Extensional/flexional angle-torque characteristics: a time-dependent, laterally directed torque $T_y(t)$ was applied following a cyclic triangular time function. After some cycles the transient process of the resulting angle oscillation $\alpha(t)$ was completed. Within each cycle a transient process occurred after each reversal of motion: this faded away with an onset time γ . Therefore, the cycle time t_c of the torque-time function had to be sufficiently long ($t_c \approx 1 \text{ min} \gg \gamma$) in order that the transient process could fade away in the first part of the respective half-characteristic and no longer could influence the subsequent larger part [11]. Then, the differential stiffness $dT_y/d\alpha$, read from this part of the characteristic,

was not influenced by the transient process and represented the actual instantaneous stiffness of the segment as the function of the flexion/extension angle (figure 2).

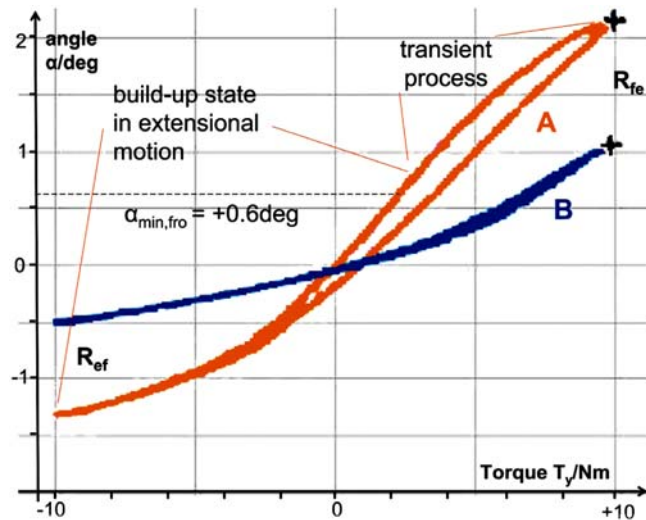


Fig. 2. Characteristics of segment L4/L5A. Torque amplitude: 10 Nm. Minimum stiffness at flexion angle $\alpha_{\min, \text{fro}} = +0.6$ deg. Parameter of force line of preload F_z corresponding to figure 3; A: central position $((x, y) = (0, 0))$, B: dorsal position $((x, y) = (-40 \text{ mm}, 0))$

Measurement of IHA-migration: the spatial resolution of the position of the moved coordinate system was $0.5 \mu\text{m}$ for the translation of its origin and 0.5 mdeg for the flexion/extension angle α . Thus, the paths of IHA-migration (centrodes) could be determined in a close approximation as the function of the angle α by using small successive angle intervals ($\Delta\alpha \leq \text{ROM}/400$). For each interval a finite helical axis (FHA) could be calculated without further ado. The successive calculated FHA-positions conformed to the IHA-positions in a close approximation and thus represented the respective centrode since the intervals were almost differentially small. Then the centrode was related to anatomical structures. The differential stiffness along the flexional angle–torque characteristics of the build-up state was related to the corresponding IHA-positions, both functions of the flexional angle α .

Range tracking: Since the angle intervals $\Delta\alpha$ used for FHA determinations depend on range of motion ($\Delta\alpha \leq \text{ROM}/400$) the set of FHA positions conform to the centrode of IHA-migration all the more because the ROM is set smaller. Therefore, the fixed coordinate system was stepwise tracked by displacements of F_z along the sagittal direction.

3. Results

First of all it should be mentioned that for the lumbar segments the direction of IHA was always nearly parallel to the applied torque vector \vec{T}_y , independent of the flexional/extensional angle α (maximal angle differences $< 10^\circ$). Additionally the screw pitch was low so that the segments carried out almost rotational or at most small helical movements like a technical screw with a low thread pitch.

Figure 2* shows two $\alpha(T_y)$ characteristics of L4/L5A segment: under the preload $F_z = 200 \text{ N}$ through the center of resistance (A) and under $F_z = 200 \text{ N}$ when its line was shifted dorsally by 40 mm (B). This force displacement was equivalent to the exerting of additional static extensional torque of 8 Nm, by which the small range of motion was tracked into the region of extended segment. Consequently, the characteristics remained asymmetric, but differential stiffness increased considerably.

Figure 3 shows the corresponding centrodes of L4/L5A. IHA migrations were found to be small in flexion and extended in extension. Under pre-extension the centrode was dorsally shifted. The centrodes ran almost parallel to the x -axis. The position of the IHA was described by the a -axis whose origin was put in the IHA-position which corresponded to minimum differential stiffness of the characteristic at $\alpha_{\min, \text{fro}} = +0.6$ deg. Each position of the IHA in both centrodes was described by its a -value and related to the differential stiffness by means of the parameter of the centrodes, the respective extensional/flexional angle α .

Figures 4 and 5 present respective measurements for L3/L4A segment. The transient process was again considerable when in reversal of motion (R_{fe}) the initial stiffness was small. The considerable asymmetry of the characteristics again corresponded to wide dorsal migrations of the IHA, also in the pre-extended segment. The centrodes for positions A or B of F_z fit

* At the reversal point (R_{fe}) from the most flexed to extensional motion the characteristic A indicated a pronounced transient process causing the hysteresis. For the characteristic B, however, the transient process was shorter and therefore the hysteresis smaller. Since the enhancement of stiffness with constant viscosity of the material shortens the time constant of a transient process, this finding mirrors the fact that the instantaneous stiffness of the segment is larger in the case B than in the case A. In both cases, the high segment stiffness at the reversal point R_{ef} shortened the transient process so that here the hysteresis was practically absent: in this way, the characteristics presented asymmetric shapes of hysteresis, altogether.

together. Note: In the extensional interval from $+0.1^\circ$ to -0.3° the IHA migrated over almost 20 mm to the back!

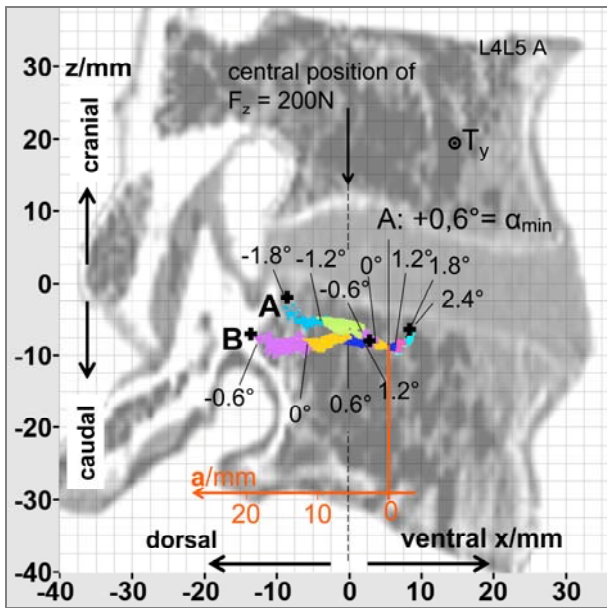


Fig. 3. CT-reconstruction of L4/L5A segment in the z - x plane and intersections of IHA in flexion/extension.

Parameter: angle of flexion. A: preload $F_z = 200$ N through the center of resistance (central position of F_z , $x = 0$). B: dorsal position of $F_z = -40$ mm. Wide IHA centres over more than 20 mm parallel to the intervertebral disc in flexing/extending motion produced by time-dependent torque T_y . Parameter along the centres is the respective extensional/flexional angle as plotted in figure 2

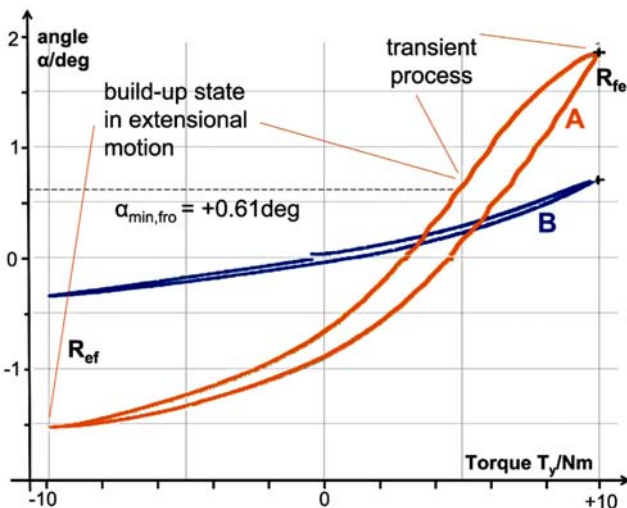


Fig. 4. Characteristic of segment L3/L4A corresponding to IHA migration in figure 5. In extensional motion, the minimum differential stiffness appeared at flexion $\alpha_{\min, \text{fro}} = 0.61$ deg. Parameter of force line of preload F_z corresponding to figure 5; A: position $((x, y) = (0, 0))$, B: dorsal position $((x, y) = (-40 \text{ mm}, 0))$

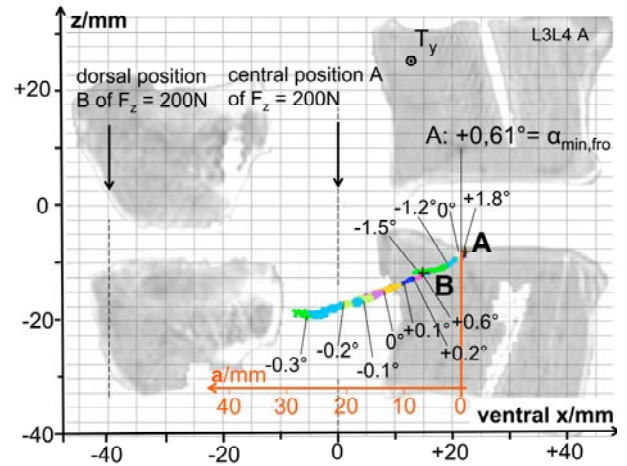


Fig. 5. CT-reconstruction of L3/L4A segment in the z - x plane and intersections of IHA in flexion/extension.

Parameter: angle of extension/flexion. In central position, F_z runs through the center of the spinal channel, in dorsal position through dorsal region of the processus spinosus. Both centres (A, B) perfectly fit into one another

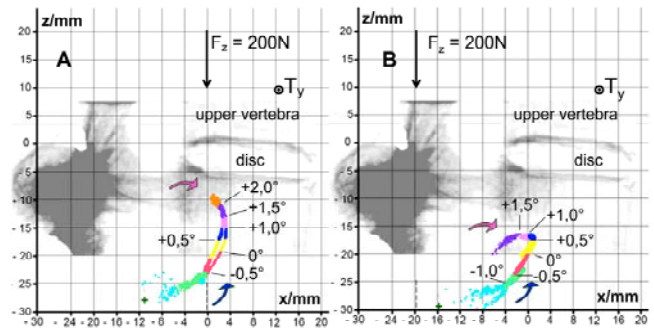


Fig. 6. Centres in flexion/extension for the thoracic segment Th2/Th3A. A: central position of the preload $F_z = 200$ N, B: dorsal position of F_z . Amplitude of oscillating torque: 4 Nm

Segments Th2/Th3A and L4/L5A originated from the same spine but showed completely differing IHA-migrations. In the two thoracic segments the IHA migrated more in caudal/cranial direction (figure 6) also for the case that the both joints were brought into function by dorsal shifting of the preload F_z . Under dorsal preload the centre (B) was slightly dorsally displaced by about 3 mm. In the angular interval from -1.0° up to $+0.5^\circ$ the centres showed almost parallel shapes.

4. Discussion and conclusions

By range tracking the considerable dorsal migration of the IHA was prolonged in all three L4/L5 and in three L3/L4 segments. All these segments had

comparable properties: a) ventral/dorsally aligned centres under central and dorsally shifted preloads, b) asymmetric characteristics, hence c) rapidly increasing the differential stiffness in extensional movement. Here the IHA-migration could be related to the non-linearity of the characteristics (figure 7). The data validated the findings of WACHOWSKI et al. [3] with further L3/L4 and L4/L5 segments whose ranges of measurements were not shifted to the regions of higher extension of the segments by static pre-extension. In one L3/L4A segment, the IHA was found to be practically stationary like it is in L1/L2 segments, in which the joint facets are almost sagittally aligned, so that the joints cannot guide extensional/flexional motions [12].

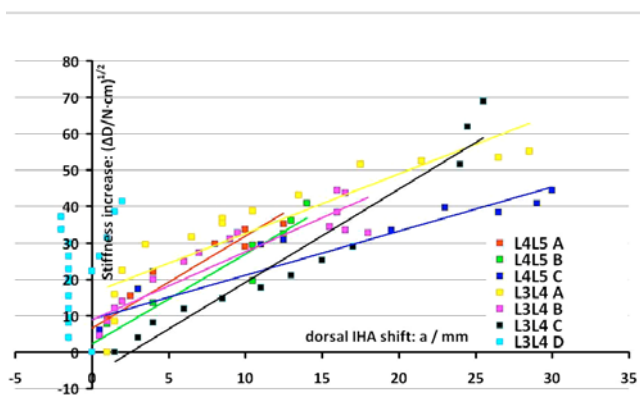


Fig. 7. Correlation of IHA-position a with instantaneous differential stiffness $D(a)$ of the segment. The relationship between $D(a)$ and IHA-position a followed the Steiner theorem in the first approximation. Only one (L3/L4D) of the segments did not show dorsal migration of the IHA

Nevertheless, by means of this dorsal IHA-motion, L4/L5 and L3/L4 segments exhibit a powerful mechanism to limit extensional motion by rapid increase of the geometric moment of inertia.

The centres of both Th2/Th3 segments took more or less caudal or cranial courses. Though the application of the Steiner theorem was not appropriate for geometrical reasons, the migration of the IHA surely made contributions to the more or less symmetric nonlinearity of the respective characteristics.

At first glance these different patterns of IHA-migration in lumbar or thoracic segments seem to be surprising since in extension the articulating surfaces of joints were in contact taking over the dominant guidance in both cases. It is, however, well-known that the curvature morphology of the articulating surfaces is oppositely shaped (figure 8): the upper and the lower facets of the lumbar/thoracic segments show, respectively, convex/concave and concave/convex contours

in sagittal cuts [12]. These qualitative anatomical findings suggest two simple models which reveal the different kinematics of the two types of segments for extension. Figure 8 illustrates this schematically. In both cases, the motion of the upper vertebra is guided by a dimeric link chain R [13], [14]: the upper vertebra can simultaneously rotate around the axis C_{lo} (defined by both facets of the lower vertebra) and around the axis C_{up} (defined by both facets of the upper vertebra). In any case, C_{lo} lies distal to C_{up} and the line $C_{lo}C_{up}$ meets the contact C of the articulating surfaces. Due to the application of dT_{ex} (extension producing torque increment) the upper vertebra with the upper joint facets rotates around the instantaneous helical axis (IHA) by the increment $d\alpha$. According to the laws of kinematics [15] IHA has to intersect the line $C_{lo}C_{up}$. The incremental rotation consists of the two incremental rotations around the morphologically given axes C_{lo} and C_{up} :

$$d\alpha = d\alpha_{lo} + d\alpha_{up}. \quad (2)$$

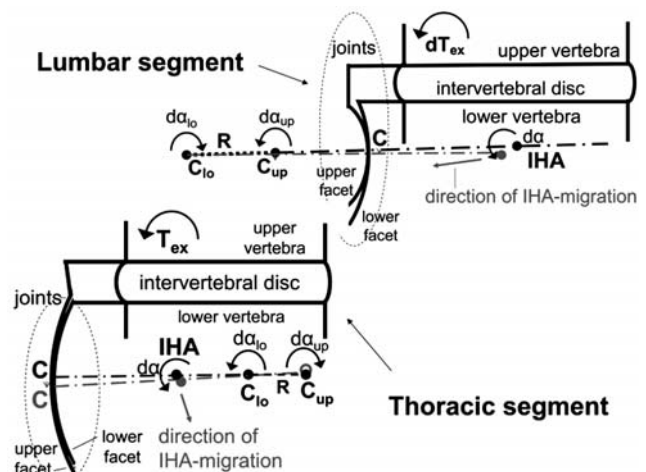


Fig. 8. Models of the joint guidance in lumbar and thoracic segments. Details in the text

The increment $d\alpha_{lo}$ describes the pivoting of the line $C_{lo}C_{up}$ around C_{lo} , which is fixed in the reference. The position of IHA is determined by the ratio:

$$\frac{d\alpha_{up}}{d\alpha_{lo}} = \frac{-r_{lo}}{r_{up}} \quad (3)$$

with r_{lo} – the distance between IHA and C_{lo} and r_{up} – the distance between IHA and C_{up} .

Lumbar segments: for neutral segment position IHA was found to be ventrally positioned in respect of the axes C_{lo} and C_{up} . Therefore the distances r_{lo} and r_{up} had the same but the incremental rotations $d\alpha_{lo}$ and

$d\alpha_{up}$ of the opposite signs. Since $r_{lo} > r_{up}$, the increment $|d\alpha_{up}| > |d\alpha_{lo}|$. Therefore the main part of extension complied with rotation around the axis of the moved articulating surface. The caudal displacement of IHA produced by the extensional rotation around C_{lo} remained small (figures 8 and also 3, 5).

Thoracic segments: since the curvatures of the articulating surfaces are small [12], the axes C_{up} and C_{lo} are ventrally positioned in relation to IHA. IHA was found for neutral flexion/extension ($\alpha = 0$) in the dorsal part of the lower vertebra segment nearby the intervertebral disc of Th3/Th4. Since $r_{lo} < r_{up}$ (figure 8), the main part extensional rotation was now given by the rotation $d\alpha_{lo}$ around C_{lo} . The wide caudal migration of the IHA indicated that the radii of curvature of the joint facets are large.

Altogether both hypotheses could be confirmed.

1. The IHA-migration largely depends on the curvature morphology. 2. Dorsal IHA-migration produces enhancement of segment stiffness.

5. Conclusions

1. The definition and resolution of IHA-migration could be increased by tracking the range of measurements.

2. IHA-migration depends on the spinal level examined, but is consistent within the same level in different specimens.

3. IHA-migration in spinal segments is determined by the curvature morphology and by the alignment of joint facets.

4. Dorsal migration of the IHA stiffens lumbar segments mainly by continuous increase of the geometric moment of inertia.

References

- [1] CRISCO J.J., FUJITA L., SPENCINER D.B., *The dynamic flexion/extension properties of the lumbar spine in vitro using a novel pendulum system*, Journal of Biomechanics, 2007, 40(12), 2767–2773.
- [2] RENNER S.M., NATARAJAN R.N., PATWARDHAN A.G., HAVEY R.M., VORONOV L.I., GUO B.Y., ANDERSSON G.B., AN H.S., *Novel model to analyze the effect of a large compressive follower pre-load on range of motions in a lumbar spine*, Journal of Biomechanics, 2007, 40(6), 1326–1332.
- [3] WACHOWSKI M.M., MANSOUR M., HAWELLEK T., KUBEIN-MEESBURG D., HUBERT J., NÄGERL H., 2009, *Parametric Control of the Stiffness of Lumbar Segments*, Strain. doi: 10.1111/j.1475-1305.2009.00686.x
- [4] WACHOWSKI M.M., MANSOUR M., LEE C., ACKENHAUSEN A., SPIERING S., FANGHANEL J., DUMONT C., KUBEIN-MEESBURG D., NÄGERL H., *How do spinal segments move?* Journal of Biomechanics, 2009, 42(14), 2286–2293.
- [5] ROUSSEAU M.A., BRADFORD D.S., HADI T.M., PEDERSEN K.L., LOTZ J.C., *The instant axis of rotation influences facet forces at L5/S1 during flexion/extension and lateral bending*, Eur. Spine J., 2006, 15(3), 299–307.
- [6] SCHNELL W., GROSS H., HAUGER W. (eds.), *Technische Mechanik*, Springer-Verlag, Berlin, Heidelberg, New York, London, Paris, Tokyo, 1989.
- [7] BEATTY M.F., *Kinematics of finite rigid-body displacements*, J. Physics Am., 1966, 34, 949–955.
- [8] FANGHANEL J., SCHULTZ F., *Mitteilung über eine Konservierungsflüssigkeit für anatomisches Präpariermaterial*, Zeitschrift für Medizinische Labortechnik, 1962, 3, 329–332.
- [9] WILKE H.J., KRISCHAK S., CLAES L.E., *Formalin fixation strongly influences biomechanical properties of the spine*, Journal of Biomechanics, 1996, 29(12), 1629–1631.
- [10] MANSOUR M., SPIERING S., LEE C., DATHE H., KALSCHUEER A.K., KUBEIN-MEESBURG D., NÄGERL H., *Evidence for IHA migration during axial rotation of a lumbar spine segment by using a novel high-resolution 6D kinematic tracking system*, Journal of Biomechanics, 2004, 37(4), 583–592.
- [11] MEYER E., GUICKING D., *Schwingungslehre*, Vieweg-Verlag, Braunschweig, 1974.
- [12] ANETZBERGER H., FRIEDLE H.P., PUTZ R., TRENTZ O. (eds.), *Posttraumatische Defekt und Infektsanierung*, Schädel, Wirbelsäule, Becken, Georg Thieme Verlag, Stuttgart, New York, 1997.
- [13] KUBEIN-MEESBURG D., NÄGERL H., FANGHANEL J., *Elements of a general theory of joints. 1. Basic kinematic and static function of diarthrosis*, Anatomischer Anzeiger, 1990, 170(3–4), 301–308.
- [14] NÄGERL H., KUBEIN-MEESBURG D., FANGHANEL J., *Elements of a general theory of joints. 7. Mechanical structures of the relative motion of adjacent vertebrae*, Ann. Anat., 1992, 174(1), 66–75.
- [15] WOLF K., *Lehrbuch der technischen Mechanik starrer Systeme*, Springer, Wien, 1947.